Bachelor Thesis

Czech Technical University in Prague

F3 Faculty of Electrical Engineering
Department of Control Engineering

Vehicle steering systems development

Filip Dašek

Supervisor: doc. Ing. Tomáš Haniš, Ph.D.
Field of study: Faculty of Electrical Engineering
May 2023

Acknowledgements

Firstly, I would like to thank my supervisor, doc. Ing. Tomáš Haniš, Ph.D., for his help and patience throughout my bachelor's thesis. Secondly, I would like to thank my friends and family that supported me throughout my bachelor's studies.

Declaration

I declare that the presented work was developed independently and that I have listed all sources of information used within it in accordance with the methodical instructions for observing the ethical principles in the preparation of university theses.

Prague, May 26, 2023

_____

Signature

Prohlašuji, že jsem předloženou práci vypracoval samostatně a že jsem uvedl veškeré použité informační zdroje v souladu s Metodickým pokynem o dodržování etických principů při přípravě vysokoškolských závěrečných prací.

V Praze dne 26. května 2023

_____

podpis autora práce

iii

Abstract

The aim of this bachelor's thesis is to briefly explore the dynamics of cars and various steering systems, including rack and pinion and worm and sector, as well as power steering systems. The steer-by-wire concept is introduced with state-of-the-art approaches and implementations. The study also describes the design and detailed implementation of a prototype steer-by-wire unit. The main objective of this research is to simulate a steering system which uses using data from the prototype steer-by-wire unit. The results of the study demonstrate the feasibility of the steer-by-wire technology in modern vehicles and its potential to enhance vehicle performance and safety. Overall, this thesis provides valuable insights into the development and application of steer-by-wire systems in the automotive industry.

Keywords: power steering unit, steer-by-wire, lateral dynamics, single-track vehicle model, control

Supervisor: doc. Ing. Tomáš Haniš, Ph.D.

Abstrakt

Cílem této bakalářské práce je stručně prozkoumat dynamiku automobilů a různé systémy řídící zatáčení kol jako je hřebenové či šnekové řízení včetně systémů s posilovačem řízení. Koncept steer-by-wire je představen s nejnovějšími přístupy a detailními implementacemi. Studie rovněž popisuje návrh a detailní implementaci prototypové steer-by-wire jednotky. Hlavním cílem této práce je pak simulovat systém řízení jak přední, tak i zadní nápravy kol pomocí dat z prototypové steer-by-wire jednotky. Výsledky studie poukazují na možnost nasazení technologie steer-by-wire v moderních vozidlech a její potenciál zlepšit výkonnost a bezpečnost vozidla. Celkově tato práce poskytuje cenné poznatky o vývoji a aplikaci systémů steer-by-wire v automobilovém průmyslu.

Klíčová slova: posilovač řízení, steer-by-wire, příčná dynamika, jednostopý model vozidla, řízení

Překlad názvu: Vývoj systému řízení vozu

Contents

v

Figures

vi

Tables

Chapter 1

Introduction

1.1 Motivation

It may seem that automotive industry doesn't have anything new to come up with other than autonomous cars. The concept of four wheel vehicle with steering wheel which turns the front wheels is known for more than century. However, this idea is clearly wrong. The way to achieve new and groundbreaking cars leads through by-wire systems.

With these systems there will be no direct physical connection with driver and vehicle control, so that the drivers fault could be erased by highly advanced control algorithms.

1.2 Thesis goals

Thesis main goals are following:

- Get familiar with vehicle dynamics and introduce the single-track vehicle model.

- Introduce steering and power steering systems.

- Implement prototype steer by wire unit and evaluate it.

- Simulate and propose the benefits of steer-by-wire systems.

1.3 Outline

This thesis is structured into seven chapters, with this introduction being the first.

The second chapter delves into various steering systems and their principles. Additionally, it introduces the concept of steer-by-wire technology.

The third chapter provides a concise overview of vehicle dynamics and presents a model that will be utilized for simulations in the sixth chapter.

The fourth chapter presents all the hardware components required to implement a prototype steer-by-wire unit.

In the fifth chapter, a detailed implementation process of the prototype steer-by-wire unit is provided.

The sixth chapter focuses on the experimental and simulation-based evaluation of the steer-by-wire unit.

Seventh chapter is the conclusion.

Chapter 2

Theory behind steering

2.1 Introduction

This chapter examines various methodologies and approaches pertaining to car steering, aiming to provide an understanding of the subject matter. It explores the evolution of steering technologies, ranging from traditional mechanical systems to the latest electronic and steer-by-wire advancements.

2.2 State of the art

In modern-day automobiles, a standard is a steering wheel directly connected to the steering mechanism through a steering column and shaft. Similarly, the electromechanical power steering system employing a rack and pinion mechanism has become a standard practice. However, in recent times, there has been a growing trend towards the adoption of steer-by-wire systems, which will be further explored in subsequent discussions, indicating their increasing prevalence in newer vehicle models.

2.3 Conventional steering mechanisms

2.3.1 Worm and sector mechanism

Worm and sector steering is a type of steering mechanism used in vehicles. It consists of a worm gear, which is a gear in the shape of a screw, and a sector gear, which is a gear with teeth on a curved surface. In this mechanism, the worm gear is turned by the steering wheel, causing it to rotate. As the worm gear rotates, it engages with the teeth of the sector gear, causing it to move along the curved surface.
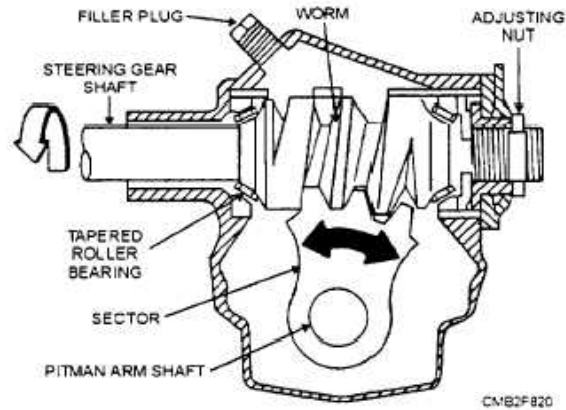
Figure 2.1: Worm and sector gear mechanism [cita]

Sector gear is attached to the pitman arm, which translates the motion to the center link, causing it to move left and right. This motion of the center link is then finally translated into wheels via tie rods connected on both sides.
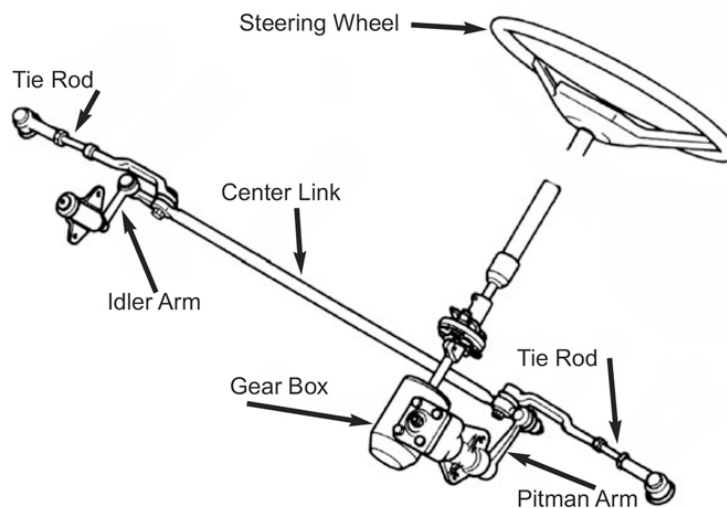
Figure 2.2: Worm and sector steering mechanism [Laz]

This mechanism is less common in modern vehicles, which often use rack and pinion steering instead.

■ 2.3.2 Other worm gear mechanisms

There exist other steering mechanisms that utilize worm gear technology, such as worm and roller, cam and lever, and worm and sector gear with recirculating balls. These mechanisms are constructed based on similar principles, which involve transmitting motion from the steering shaft to the pitman arm and center link. For this reason, a detailed explanation of these mechanisms will not be provided.

■ 2.3.3 Rack and pinion mechanism

Rack and pinion steering is a common type of steering mechanism used in modern vehicles. It consists of a pinion attached to the steering column and a long rack with teeth running along its length. In this mechanism the pinion gear rotates as driver turn the steering wheel. Rotating pinion then engages with the teeth on the rack. This causes the rack to move left and right. This motion is then translated into the movement of the vehicle's wheels as it was in the case of worm and sector steering mechanism. The difference is that the center link is subtituted with the rack.
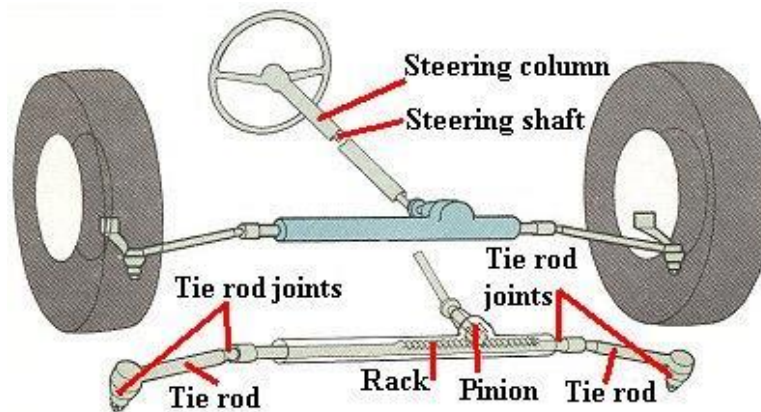
Figure 2.3: Rack and pinion steering mechanism [citc]

Rack and pinion steering offers several advantages over other types of steering mechanisms [Dru22]. Firstly, it is very precise. It is also relatively simple and lightweight, making it easy to incorporate into modern vehicles. However, there are some downsides to rack and pinion steering as well. It can be more expensive to manufacture. Additionally, the rack can wear out over time, which can result in increased maintenance costs. Overall, rack and pinion steering is a reliable and effective mechanism that has become the standard in modern vehicles. Its precision and ease of use make it a popular choice among drivers and manufacturers alike.

■ 2.4 Power steering mechanisms

Power steering is a system that assists drivers in turning the wheels of their vehicle. It is designed to reduce the amount of effort required to turn the wheels, making it easier for the driver to control the vehicle, especially at low speeds or when parking.

■ 2.4.1 Hydraulic power steering

Hydraulic power steering is a system that uses hydraulic fluid to help drivers steer their vehicles. The system consists of a power steering pump, which is

driven by a belt connected to the engine, and a series of hydraulic lines that connect the pump to the steering gearbox or rack. When the driver turns the steering wheel, a valve in the steering gearbox or rack redirects the hydraulic fluid, which increases the pressure on one side of the steering mechanism and reduces it on the other. This creates a force that helps the driver turn the wheels.
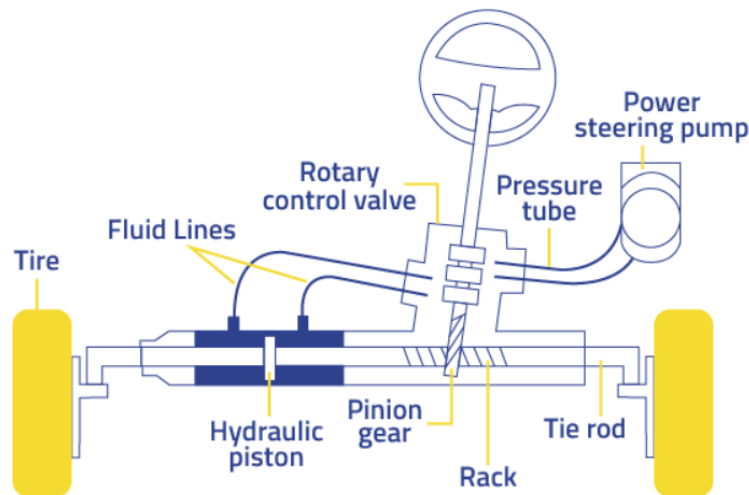
Figure 2.4: Hydraulic power steering [Bha]

2.4.2 Electrohydraulic power steering

Electrohydraulic power steering is a hybrid system that combines hydraulic power steering with electronic control. Instead of a traditional hydraulic pump, an electric motor drives a hydraulic pump to generate the hydraulic pressure needed to assist the driver's steering efforts.

2.4.3 Electromechanical power steering

Electromechanical power steering (EPS) is a system that uses an electric motor to assist the driver's steering efforts instead of the traditional hydraulic pump used in hydraulic power steering systems. EPS systems use an electric motor and gear system to provide the steering assistance. This gear is typically mounted either on the steering wheel column or on the steering gearbox, which is commonly a rack-and-pinion system. The amount of assistance is controlled by an electronic control unit (ECU) that receives information from various sensors, including the vehicle speed, steering angle, and torque applied to the steering wheel. The ECU then adjusts the motor's power output to provide the appropriate level of steering assistance.
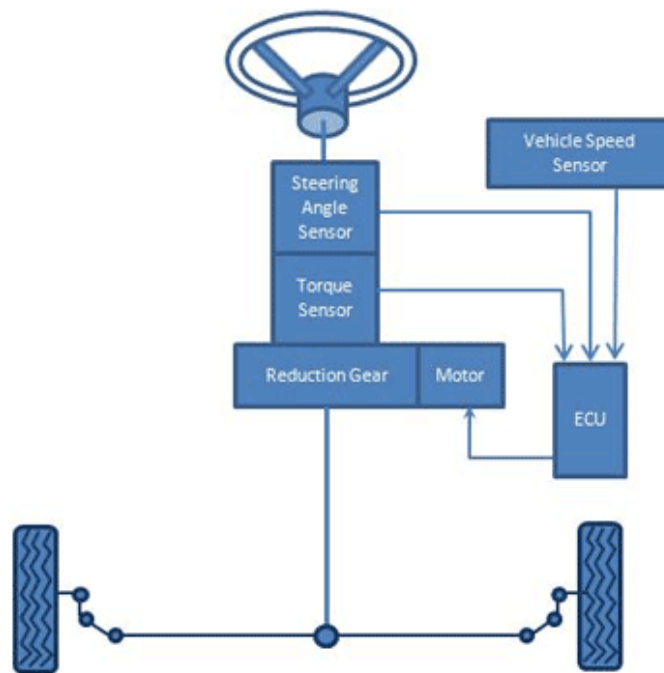
Figure 2.5: Electromechanical power steering [citb]

EPS systems are becoming more popular in modern vehicles due to their efficiency and adjustability [Fir22]. However, lots of drivers complain that EPS systems do not provide the same level of "response from the wheels" as hydraulic power steering systems.

2.5 Steer by wire

2.5.1 Introduction

Steer-By-Wire (SBW) is a revolutionary technology that aims to replace traditional mechanical linkages between the steering wheel and the wheels with electronic control systems. Instead of a physical connection, steer-by-wire systems use sensors, electric motors, and computer algorithms to control the direction of the vehicle. While this technology has the potential to offer numerous benefits such as increased fuel efficiency, enhanced safety features, and greater design flexibility, it also presents several significant challenges. In this context, this technology must overcome a range of technical, regulatory, and social obstacles to achieve widespread adoption.

2.5.2 State of the art aproaches

The Infiniti Q50 was one of the earliest mass-produced cars to feature SBW technology, with its implementation dating back almost ten years. Alex Davies, in his article on the Q50 [Dav14], highlights the improved response and precision of the steering system compared to a mechanical setup. He also

notes additional benefits, such as minimizing vibrations from the road that could disturb the driver and enhancing the car's active lane control system. However, it is important to mention that the Q50 still retains a mechanical connection as a backup in the event of SBW control unit failure.

According to the information provided in Perkins' article [Per23], the latest Lexus RZ450e model eliminates the mechanical connection entirely. The mechanical steering construction remains the same as in conventional cars, with an electric motor connected to the rack and pinion mechanism, which, in turn, moves the tie rods that rotate the wheels. The main difference lies in the replacement of the traditional steering column with wires.

To ensure redundancy and enhance safety, the steering system incorporates duplicate components. In the event of a component failure, a backup component is available. The SBW unit is powered by a 400 V battery, which is responsible for powering the traction motors. Redundancy in power delivery is achieved by connecting the SBW system with the car's 12 V battery. Additionally, a small lithium-ion battery is specifically dedicated to the SBW system in case of a the 12 V battery failure.

The Lexus SBW system exhibits more sensitive wheel movements at lower speeds compared to higher speeds. This sensitivity enhances maneuverability and comfort during low-speed maneuvers while providing increased stability during high-speed maneuvers.

Figure 2.6: Lexus RZ450e [citd]

Chapter 3

Vehicle dynamics

3.1 Introduction

The examination of vehicle dynamics will start at the vehicle wheel. With obtained informations about the wheel dynamics the attention will pass to two wheel single-track model.

3.2 Vehicle wheel

This section highly draws from book by Hans B. Pacejka [Pac02]. The basic quantities and principles of vehicle wheel dynamics are introduced here. Firstly, all the significant physical quantities of the wheel dynamics are shown if figure 3.1.
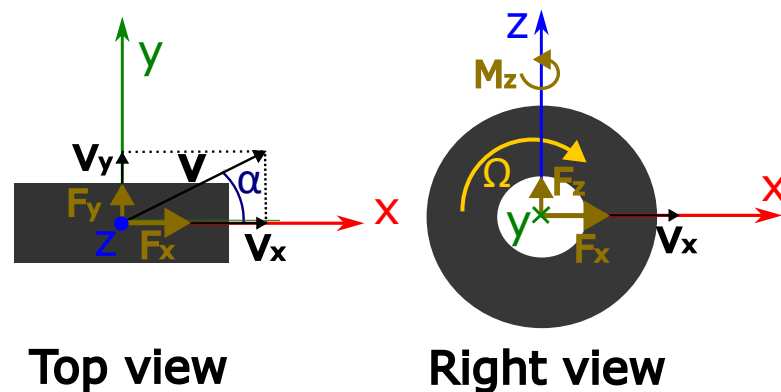
Figure 3.1: Vehicle wheel with described physical quantities

First quantity is the velocity v which could be divided into velocity in x and y axis (v_x resp. v_y). The angle between these partial velocities is named slip angle (α). Another significant physical quantity is the angular velocity of the wheel (Ω). Finally the most significant quantities in terms of dynamics are forces and torques. In this case the longitudinal, lateral and vertical forces are presented as F_x resp. F_y resp. F_z. Last but not least is the aligning torque M_z.

In the brief analysis of wheel dynamics, focus drops on the lateral and longitudinal forces. Vertical forces will not be considered. Firstly, if when a wheel rolls freely on the ground, Ω_0 is defined as the angular velocity of this freery rolling wheel. If torque in the y axis is applied on the wheel by brakes or engine, a change in the angular velocity Ω appears. With this approach a longitudinal slip κ defined in following equation arises.

$$\kappa = \frac{\Omega - \Omega_0}{\Omega_0} \tag{3.1}$$

In general, the lateral force and aligning torque are function of camber angle which is the angle of the wheel in its x axis. For purpose of this investigation this angle is not considered. In the following set of equations are linearized functions which describe the dependence of longitudial force, lateral force and aligning torque on the longitudinal slip and slip angle.

$$F_x = C_{F\kappa}\kappa, \tag{3.2}$$

$$F_y = C_{F\alpha}\alpha, \tag{3.3}$$

$$M_z = C_{M\alpha}\alpha. \tag{3.4}$$

As equations 3.2, 3.3 and 3.4 displays, the longitudinal force depends on longitudinal slip and lateral force with aligning torque depends on slip angle. Coeficients $C_{F\kappa}$ and $C_{F\alpha}$ are called longitudinal resp. lateral stifness and $C_{M\alpha}$ is called aligning stifness. This fact is of course not true in general. All of these quantities are highly nonlineary depended on both longitudinal slip and slip angle. However, in linearized model, where slip angle and longitudinal slip acquires small values, stated equations are telling a lot about the tire dynamics.

Several tire models provide a nonlinear estimation of the forces acting on the vehicle tire based on the slip angle. One such well-known model is the simplified Pacejka Magic Formula [Pac02]. A version of this formula, which describes the behavior of lateral force can be described as follows:

$$F_y(\alpha) = D\sin(C\arctan(B\alpha - E(B\alpha - \arctan(B\alpha)))), \tag{3.5}$$

where B, C, D, E are coeficients dependent on vertical force F_z and tire friction coeficients.

▍ 3.3 Single-track model

For further investigation of the vehicle dynamics, a single track vehicle model is introduced with help of already mentioned book [Pac02] and work of Denis Efremov [Efr20].

◼ 3.3.1 Assumptions

This single track model consist of two connected wheels. A few assumptions are made such as:

- Considered wheels are firmly connected.

- Each of the wheels has its own axle.

- The mass of considered model is concentrated into single Centre Of Gravity (COG).

- Only a planar motion of the vehicle is considered. Therefore no pitch, roll or vertical motions could occur.

- Aligning torque on the wheels is neglected.

◼ 3.3.2 Description of single track model quantities

The model could be seen in figure 3.2.
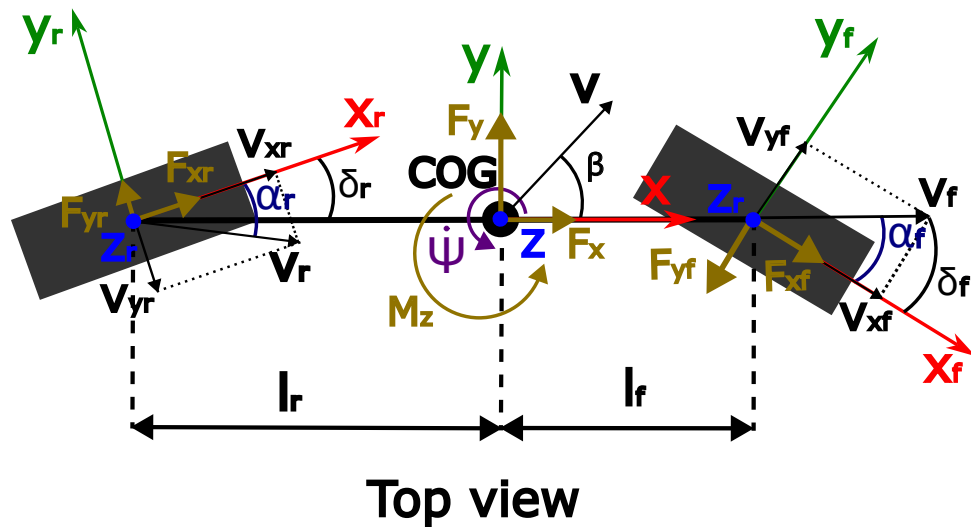
Figure 3.2: Single-track vehicle model

In the figure, some new quantities appears, such as δ_f and δ_r, which stands for steering angle of the front and rear axle, COG is the earlier mentioned centre of gravity, v is the velocity of the COG, β is the side slip angle, l_f and l_r is distance of COG and front resp. rear axle and finally $\dot{\psi}$ is the yaw rate. Also a few indexes f and r which stands for front and rear axle, appeared in the figure.

11

3.3.3 Degrees of freedom

After the set of assumptions that were made in chapter 3.3.1, a rigid body model with three degrees of freedom is expected. These degrees of freedom are velocity v, side slip angle β and yaw rate $\dot{\psi}$. Equations that describe the motion in these three degrees of freedom are listed below:

$$\dot{\beta} = \frac{1}{mv}\left(-F_x \sin\beta + F_y \cos\beta\right) - \dot{\psi}, \tag{3.6}$$

$$\dot{v} = \frac{1}{mv}\left(-F_x \cos\beta + F_y \sin\beta\right), \tag{3.7}$$

$$\ddot{\psi} = \frac{1}{I_z}M_z, \tag{3.8}$$

here I_z stands for moment of inertia in the vehicle z axis.

3.3.4 Dynamics dependency on steering angles

As expected, the steering angles have a fundamental effect on vehicle dynamics. Especially in terms of lateral dynamics. A direct projection that translates forces from the wheels to the forces and torque acting on vehicle rigid body is represented in following set of equations:

$$F_x = F_{xf}\cos\delta_f - F_{yf}\sin\delta_f + F_{xr}\cos\delta_r - F_{yr}\sin\delta_r, \tag{3.9}$$

$$F_x = F_{xf}\sin\delta_f + F_{yf}\cos\delta_f + F_{xr}\sin\delta_r + F_{yr}\cos\delta_r, \tag{3.10}$$

$$F_x = F_{xf}l_f\sin\delta_f + F_{yf}l_f\cos\delta_f - F_{xr}l_r\sin\delta_r - F_{yr}l_r\cos\delta_r. \tag{3.11}$$

3.3.5 Steering servo model

In this chapter will be introduced the model which is used for simulations in the chapter 6. The model incorporates a single-track vehicle model from [Efr20] in conjunction with the identified model of the SBW unit 5.3. The simulink scheme of the implemented model depicted below.
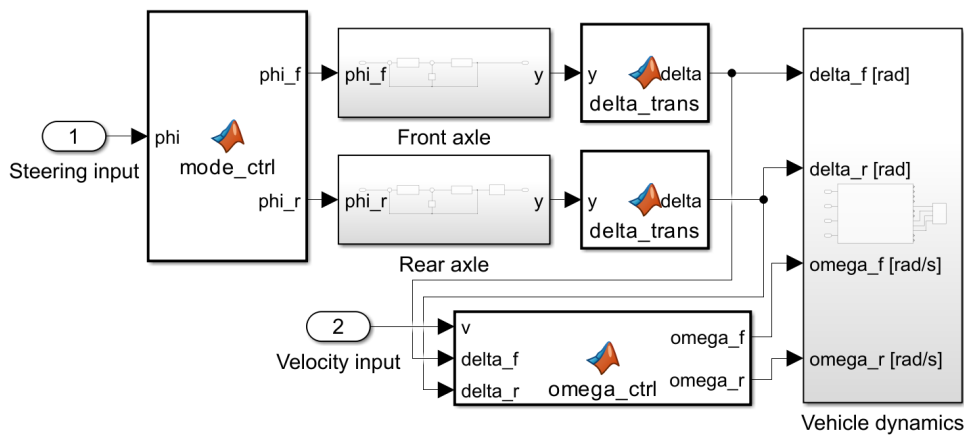
Figure 3.3: Simulink scheme of implemented model

The output of the steering system is transformed using an approximation of the real measured values from 5.2.3. The mode controller is responsible for configuring and managing the three modes discussed in chapter 6.

The values of the quantities used in the single-track model are listed in the table below:

Quantity	Symbol	Value	Unit
Mass of the COG	m	1200	kg
Moment of inertia in the z axis	I_z	2688	kg·m^2
Distance of front axle and COG	l_f	1.4	m
Distance of rear axle and COG	l_r	1.6	m
Radius of vehicle wheel	p	0.33	m

Table 3.1: Values of quantities used single-track model

Chapter 4

SBW hardware

4.1 Introduction

This chapter provides a detailed description of all the hardware components used in the implementation of the prototype SBW unit. A significant portion of these components has been taken from actual automobiles, as the automotive industry places a strong emphasis on durability and reliability.

4.2 Power steering unit

The primary hardware component required for the implementation of the SBW unit is undoubtedly the Power Steering Unit (PSU). This unit must be capable of steering the car's wheels without driver intervention. Due to the absence of a conventional steering column, the use of a PSU mounted on the steering column was not possible. Consequently, an electromechanical PSU sourced from a Citroen C3 2002 was employed. This PSU incorporates a rack and pinion steering mechanism, featuring a DC servo motor connected onto the pinion via gearbox to deliver the necessary steering force. The use of this mechanism is ideal due to its availability, compact design, and, most importantly, the capability to directly access the DC motor through an external power cable.

Figure 4.1: Used power steering unit

◼ 4.3 Motor controller

In order to operate the DC motor discussed in the previous section, a motor controller was required. For this purpose, an available Escon 50/5 servocontroller was utilized. This controller fits to control the PSU due to its ability to drive DC motors, supporting power capacities of up to 250 W. Notably, the controller incorporates an internal PI regulator that controlls the magnitude of current through the motor. This current is externally set via the duty cycle of PWM or an analog voltage magnitude.
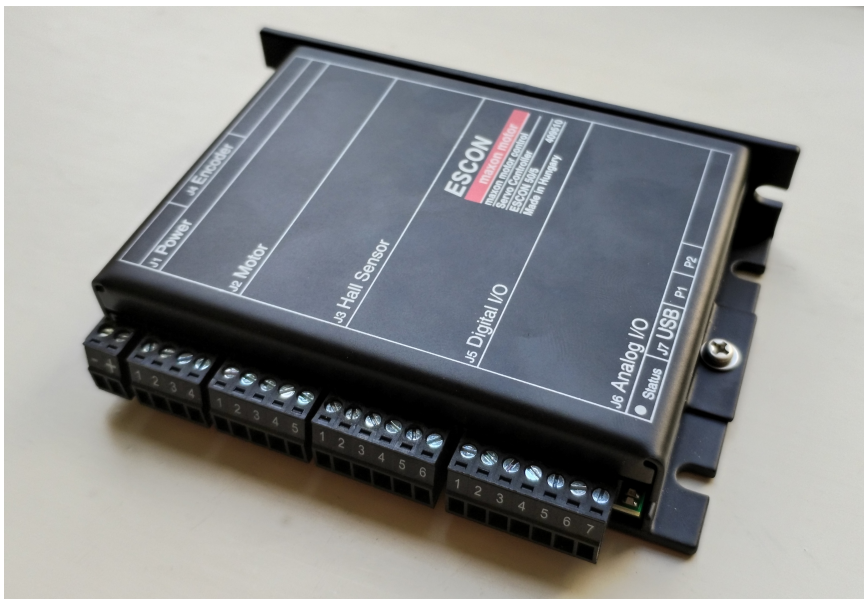
◼ 4.4 Processing unit

For data processing and PSU control a processing unit was needed. For this purpose the Texas Instruments LAUNCHXL-F28379D development board was selected. The core of this board is 32-bit TMS320F28379D MCU that has support in Matlab Simulink, which is one of the two main reasons for utilization. The second primary criterion for selecting this specific development board is its support for two Controller Area Network (CAN) bus interfaces, which are widely used as standard for communication in the automotive industry.

◼ 4.5 Steering wheel angle sensor

To gather information regarding angle of the steering wheel and the PSU, a steering wheel angle sensor from Renault Laguna II 2001-2005 was used. The utilization of this sensor was caused by the previously mentioned robustness
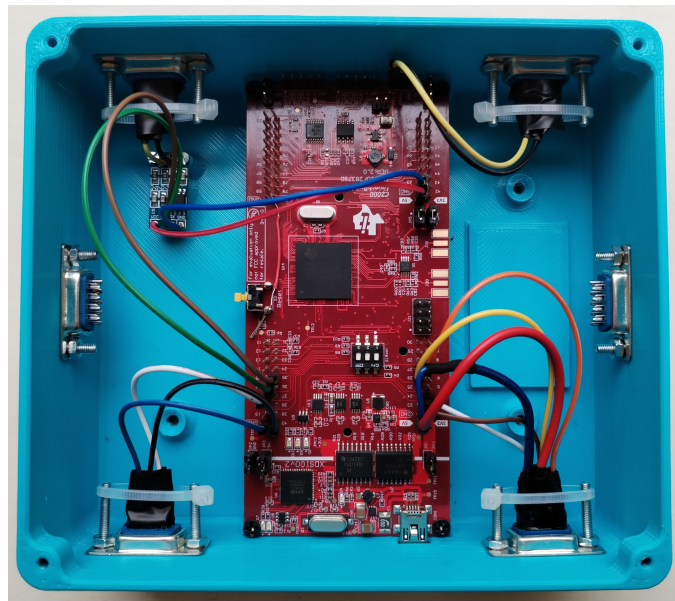
Figure 4.2: Used processing unit in 3D printed case
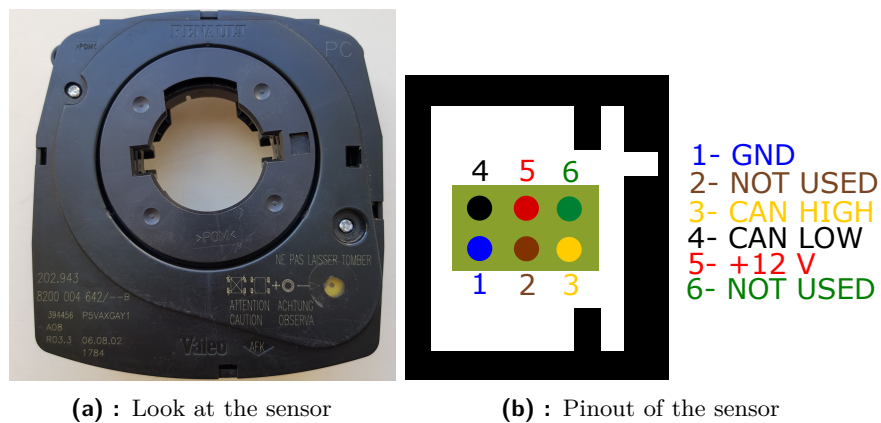

(a) : Look at the sensor   **(b) :** Pinout of the sensor

Figure 4.3: Steering wheel sensor

of automotive vehicle components. This sensor employs optical encoder technology to measure the absolute angle of the steering wheel. The pinout configuration of the sensor connector can be observed in figure 4.3b.

The sensor communicates its current absolute angle every 10 milliseconds using the CAN bus. The message produced by this sensor carries the identifier 0x0C2 and comprises eight data bytes. The first two data bytes carries the desired information in little-endian integer representation. For more detailed information, please refer to figure 4.4. When a 12 V power source is connected to the sensor, it does not produce any meaningful information until the sensor undergoes rotation such that the optical encoder can read a valid angle. The fact that the sensor requires this routine is conveyed through the first four data bytes as 0x00, 0x08, 0x00, 0x08. The sensor's range spans from -990 to 990 degrees. If the sensor's rotation exceeds either of these thresholds, the

17
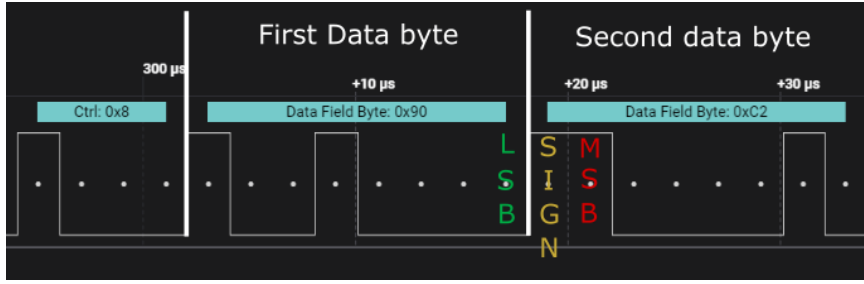
Figure 4.4: Detail of CAN message produced by the sensor

data bytes are filled in the same manner as during startup. This error state persists until the power source is disconnected. As illustrated in figure 4.5, the measured sensor characteristic represents a linear function. Equation that displays an least squares aproximation of this function is displayed below:

$$Out = 22.868\varphi, \tag{4.1}$$

here φ stands for the angle of the sensor in degrees and Out is the output value produced by the sensor.
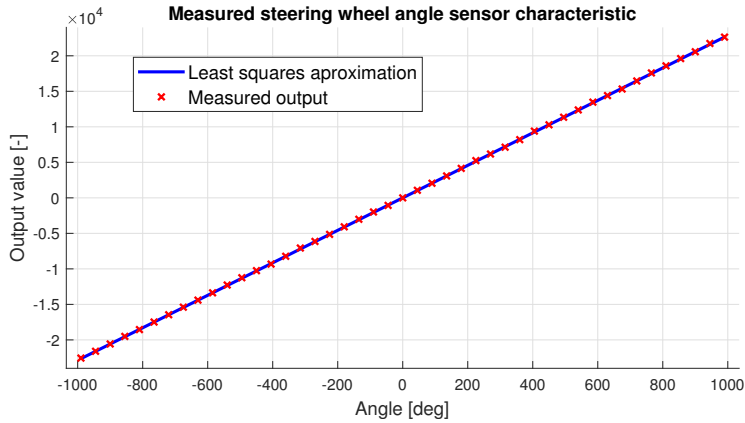
Figure 4.5: Measured characteristic of the steering wheel sensor

4.6 Wheel angle sensor

In SBW technology, significant emphasis must be placed on redundacy due to the elimination of the physical connection between the driver and vehicle's wheels. As a result, it is necessary to measure the position of the tie rod as a part of ensuring redundacy. To fulfill this requirement, an axle height sensor was used.

The sensor in question is, in fact, an angle sensor. It operates on a 5 V power supply. As an output, this sensor delivers an analog signal. The transfer characteristic of the sensor was measured and can be observed in figure 4.7. In the range of -30 - 30 degrees an affine least squares aproximation

(a) : Look at the sensor

(b) : Pinout of the sensor
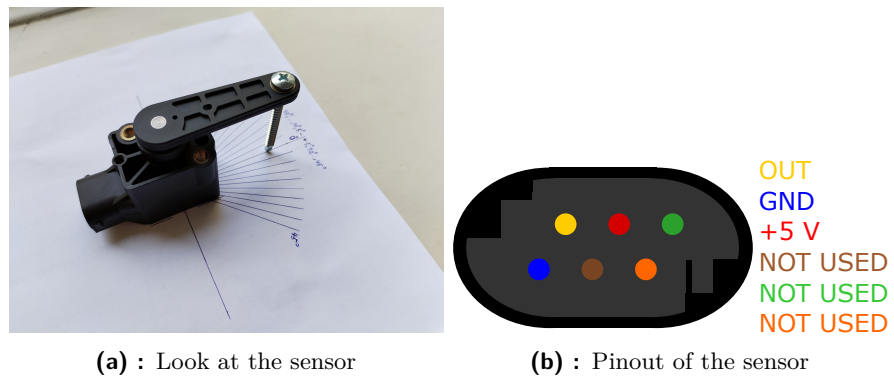
Figure 4.6: An axle height sensor
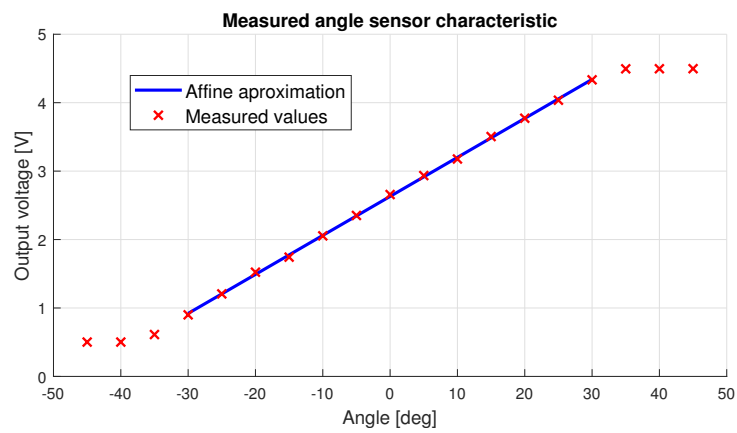
Figure 4.7: Measured characteristic of the angle sensor

of the measured sensor characteristic was made. Result of this aproximation is listed below:

$$V_{out} = 0.0570\theta + 2.631, \tag{4.2}$$

where θ is the angle of the sensor in degrees and V_{out} is the output voltage in volts.

19

Chapter 5

The SBW unit implementation

5.1 Introduction

Chapter 4 provided an introduction to all the hardware that was utilized. The focus will now shift towards examining the implementation of the prototype SBW unit.

5.2 SBW unit overview

This section provides an introduction of mechanical and electrical arrangement of implemented SBW unit.
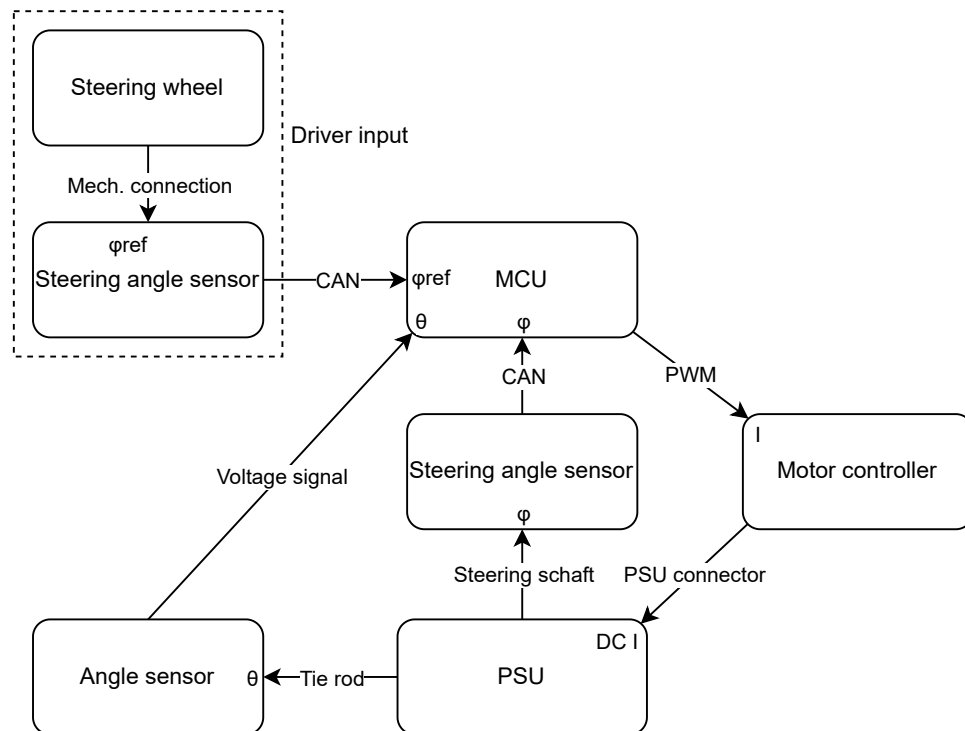
Figure 5.1: Block diagram of the SBW unit

5.2.1   Steering wheel angle measurement

To obtain the reference steering angle, the steering angle sensor introduced in section 4.5 was utilized. The sensor is rotated using a mounted 3D-printed steering wheel.

(a) : Realisation   **(b) :** 3-D model of steering wheel

Figure 5.2: Steering wheel unit used for reference measuring

5.2.2   PSU steering shaft angle measurement

The chosen system output was determined to be the angle of the steering shaft. Consequently, the steering angle sensor was affixed to the PSU as depicted in figure 5.3.
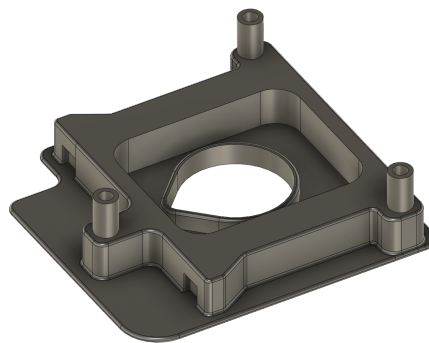
(a) : Realisation   **(b) :** 3-D model of sensor holder

Figure 5.3: Measuring of angle on the steering shaft

5.2.3   Wheel steering angle measurement

As discussed in 4.6, an angle sensor has the capability to insert redundancy into implemented SBW unit by measuring the position of the tie rod. However,

(a) : Bottom part   **(b)** : Top part

Figure 5.4: 3-D models of mechanical connection parts

for the purposes of simulation in this thesis, the steering angle of the steering shaft, denoted as φ, needs to be transformed into the steering angle of the axle, denoted as δ. The angle sensor was employed to measure this dependency.The connection of this sensor on the PSU can be observed in figure 5.5.

Figure 5.5: Connection of angle sensor on the PSU
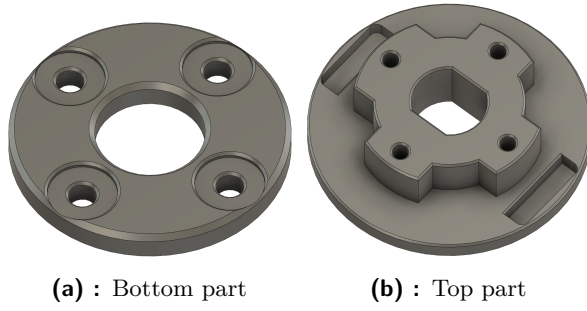
The measured characteristic showing the dependency of the sensor's output voltage on the angle of the steering shaft can be observed in figure 5.6. As depicted in the figure 5.6, the measured values were approximated using an affine function denoted as $f_{\varphi 2V}(\varphi)$. The transformation from the steering angle of the steering shaft, φ, to the steering angle of the axle, δ, can be described by the following equation:

$$\delta(\varphi) = f_{\delta 2V}^{-1}(f_{\varphi 2V}(\varphi)). \tag{5.1}$$

In the equation mentioned above, $f_{\varphi 2V}(\varphi)$ represents the previously discussed function, while $f_{\delta 2V}^{-1}(V)$ represents the inverse of the approximating function discussed in section 4.6, which pertains to the introduction of the angle sensor.

23
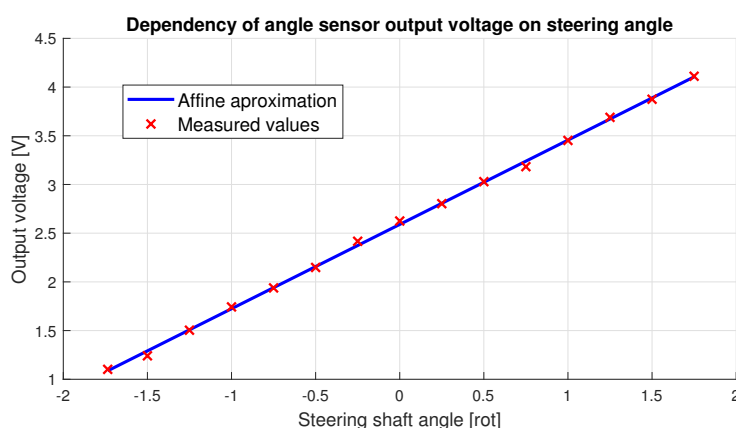
Figure 5.6: Measured values and aproximation of sensor output dependency

After neglecting an additive constant, the final transformation function that converts the output of the identified system 5.3 to the axle steering angle can be expressed as follows:

$$\delta(\varphi) = 15.188\varphi \text{ deg.} \tag{5.2}$$

5.2.4 Controllig of DC servo

The control of the DC servo motor, which is an integral component of the PSU, is accomplished using the motor controller referenced in section 4.3. The desired value of the current through the DC motor is set by the MCU via a PWM duty cycle, as illustrated in equation 5.3.

$$I_{set} = (DUTY\ CYCLE - 50\,\%)\,\frac{5}{40}\,[\text{A}] \tag{5.3}$$

Here, the *DUTY CYCLE* is expressed as a percentage value. The range of the valid PWM duty cycle is defined as 10 % to 90 %. If either of these thresholds is exceeded, the motor controller goes into an error state. The controller returns to the standard mode of operation once the duty cycle is within the specified limit.

5.3 Identification

For identification a current step response was used. The response is shown in figure 5.7. The current step has been applied in time 0 s. From this step response was identified integrating second order system with following transfer function.

$$G = \frac{k}{s(Ts + 1)} \tag{5.4}$$

Constants k and T were found as follows. Firstly an angular speed was counted by method described in section 5.4.2. From this angular velocity was determined time interval in which angular velocity has settled. Secondly a
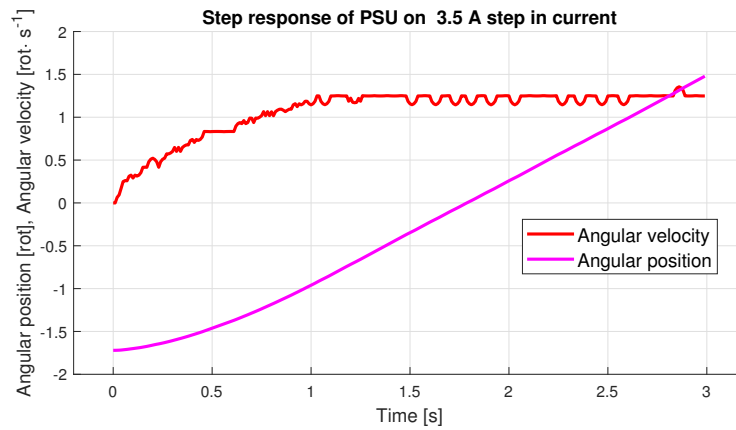
Figure 5.7: Response of PSU on 3.5 A step in current

least squares affine interpolation of measured angle in found time interval was made. The result asymptot of this interpolation is shown in following equation.

$$y = at + b = 1.228t - 2.136 \tag{5.5}$$

With use of this interpolation a constant k was defined to be equal to found parameter a. Then constant T was defined as a time difference between the step input (0 s) and time when the mentioned affine interpolation reaches angle value of system before step current was applied. Details of the identification are shown in figure 5.8. Transfer function of identified system is displayed in equation 5.6.
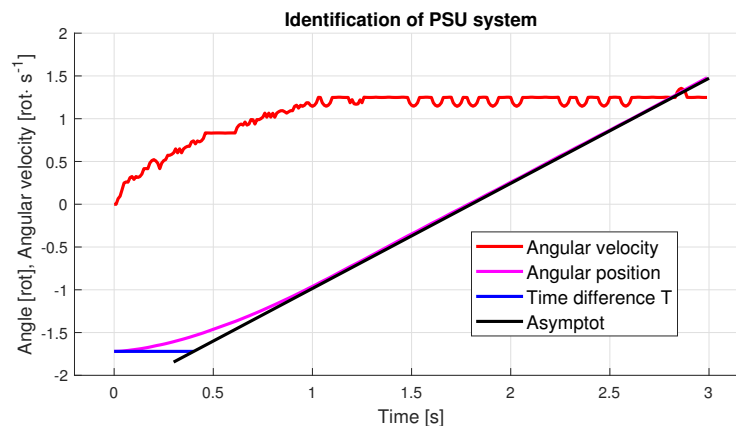
Figure 5.8: Identification of PSU system

$$G = \frac{1.228}{s(0.4198s + 1)} \tag{5.6}$$

A comparison of identified and real system is shown in following figure:

25
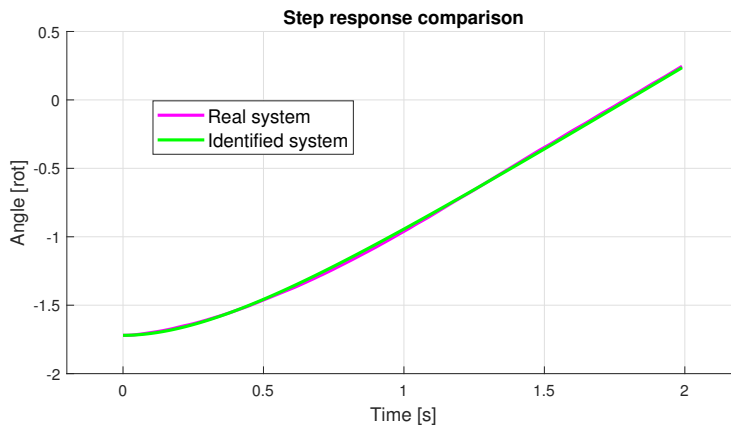
Figure 5.9: Comparison of identified and real system

5.4 Control loop

In this section, an introduction is provided for a low-level simulink control loop. The structure of this control loop is depicted in figure 5.10. This control
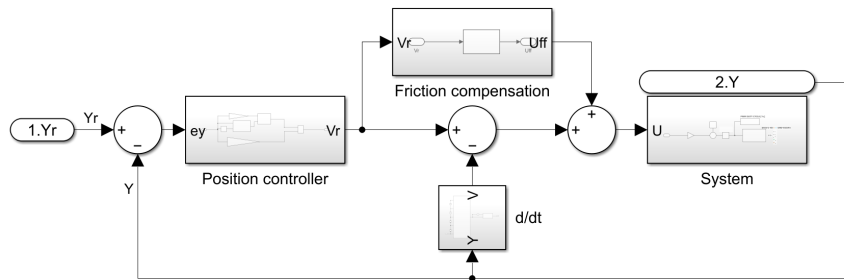
Figure 5.10: Low level simulink control loop

loop incorporates feedback control, which is widely recognized as a crucial element for effectively controlling dynamic systems, as emphasized in the book by Gene F. Franklin [GFF06]. Input and output of controlled system is discussed in sections 5.2.1 and 5.2.2.

5.4.1 Controllers

The control loop consists of two controllers, with the first and primary one being the feedback position controller. Due to the presence of significant static friction in the controlled system, a feed forward friction compensator, as described in [Col21], was employed. A comprehensive discussion on the implementation of these controllers can be found in Section 5.5.

◾ 5.4.2 Angular velocity computation

Within the control loop, the computation of the angular velocity $\dot{\varphi}(t)$ is required. To fulfill this objective, the backward difference method, as represented by equation 5.7, was employed.

$$\dot{\varphi}(t) = \frac{\varphi(t) - \varphi(t-1)}{h} \tag{5.7}$$

Here, the symbol h represents the quantization step of 0.01 seconds. Unfortunately, this method resulted in substantial s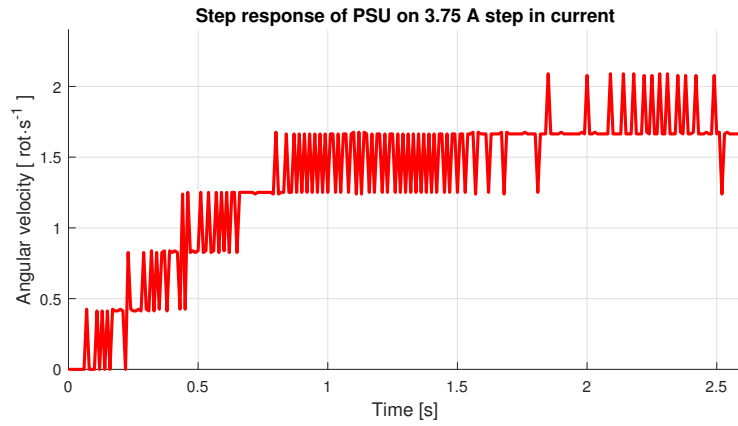pikes in the angular velocity, characterized by discrete steps which are not expected in the PSU system. For further insights, please refer to figure 5.11.

Figure 5.11: Angular velocity counted with raw sensor data

The identified issue was examined and determined to be due to the low resolution of the angular sensor. Consequently, a Gaussian smoothing technique, as outlined by Regmi [Reg21], was implemented to address this concern. In this process, each angle sample is computed as a weighted average using a Gaussian kernel. The weights within the kernel are determined by the following equation:

$$K(x^*, x_i) = \exp\left(-\frac{(x^* - x_i)^2}{2b^2}\right), \tag{5.8}$$

here, the symbol x^* represents the position within the kernel, while x_i denotes the reference position with the highest weight. The parameter b represents the width of the kernel. A specific value of x_i is not significant for the computation of kernel values. However, the value of b is crucial and was determined experimentally to be 2. Utilizing equation 5.8 with $x_i = 0$ and $b = 2$, a kernel in table below was calculated.

x^*	-2	-1	0	1	2
$K(x^*)$	0.6065	0.8825	1.0000	0.8825	0.6065

**Table 5.1:** Counted Gaussian smoothing kernel

27

When performing data smoothing, it is essential to utilize a normalized kernel. As a result, the final normalized Gaussian smoothing kernel is presented in the table below.

x^*	-2	-1	0	1	2
$K_n(x^*)$	0.1525	0.2218	0.2514	0.2218	0.1525

Table 5.2: Normalized Gaussian smoothing kernel

Now every sample of angular possition is weighted mean of last five measured angle samples as shown in equation 5.9. This angle value is then used for the calculation of angular position. The result of this smoothing technique is compared in figure 5.12.

$$\varphi_{smooth}(t) = \varphi(t)K_n(2) + \varphi(t-h)K_n(1) + \cdots + \varphi(t-4h)K_n(-2) \quad (5.9)$$
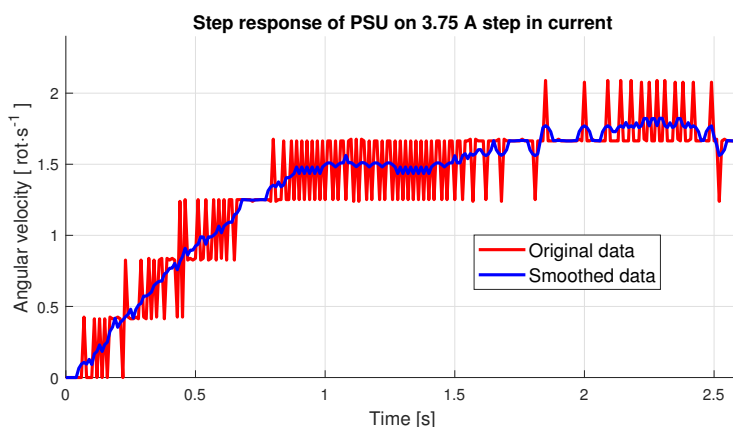
Figure 5.12: Angular velocity counted with with gaussian smoothing

5.5 Controllers in the loop

This section describes the design of previously mentioned controllers in section 5.4.1.

5.5.1 Position controller

The feedback position controller was designed using frequency-based methods. These methods were applied to the identified system, characterized by the transfer function specified in equation 5.6. The objective was to design a PI regulator by incorporating concepts from the previously mentioned book [GFF06]. Initially, the cutoff frequency at which the system's amplitude-frequency characteristic is -3 dB was determined as $f_c = 1.5, \mathrm{rad \cdot s^{-1}}$. Subsequently, a pole at the origin (integrator) was incorporated into the controller.

To achieve a PI regulator, a zero was placed at approximately one-tenth of the cutoff frequency. Finally, the controller gain was set to 1.2234 to obtain a Phase Margin (PM) of 55 degrees, while the Gain Margin (GM) was infinite.

As depicted in figure 5.13 (red color), an integrator wind-up phenomenon is observed. Consequently, an anti-wind-up control strategy, based on the article of Peterson [Pet20], was implemented. The output of the integrator is saturated when it reaches the maximum allowable control action. Additionally, the integrator output is reset whenever the absolute value of the position error $|E_r|$ falls below 0.1 rotations. The effectiveness of the anti-wind-up implementation can be observed in figure 5.13 (green color).

The next design approach involved utilizing negative feedback of the angular velocity of the output . As expected, this approach resulted in significant reduction of overshoot, as illustrated by the blue color in figure 5.13.

Finally, after successfully reducing the overshoot, the gain of the controller was multiplied by 2. The step response of the system with the designed regulator can be observed in figure 5.13 represented by the magenta color.
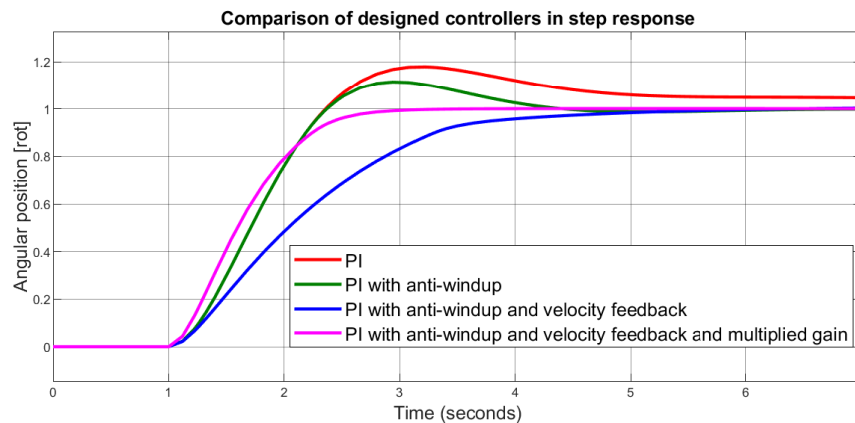
Figure 5.13: Comparison of designed controllers

5.5.2 Friction compensator

The idea from the mentioned article [Col21] was employed for friction compensation. This compensation method relies on feed-forward control. To implement this controller, the relationship between angular velocity and the current flowing through the DC servo motor of the PSU was measured. Based on these measurements, a function approximating this relationship was calculated. The function, along with the measured values, is presented in figure 5.14. The obtained approximating function was inverted and utilized as the feed-forward compensator, as depicted in figure 5.10.
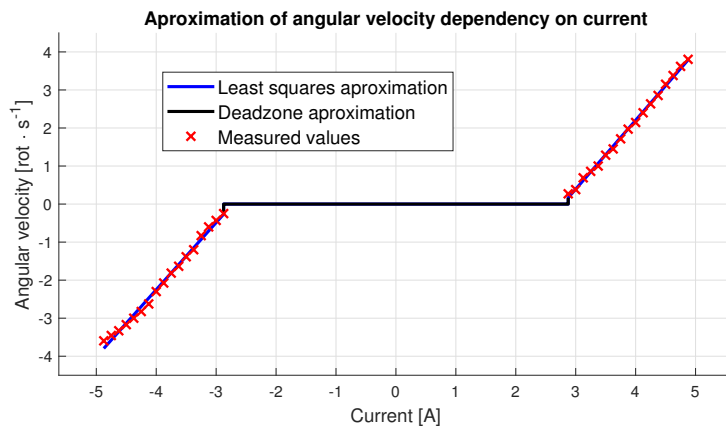
Figure 5.14: Dependency of angular velocity on current

Chapter 6

Evaluation

6.1 Introduction

The evaluation will be conducted in two distinct parts. Firstly, an experimental evaluation of the implemented SBW unit will be presented. This evaluation aims to provide practical insights into the functionality of the implemented SBW system. Secondly, a simulation utilizing a single track model and the identified system from section 5.3 will be performed. The simulation serves to demonstrate certain advantages of SBW in rear axle steering systems, as discussed in the bachelor's thesis authored by Jan Belák [Bel20].

6.2 Experimental evaluation

An experimental evaluation of the SBW unit uses two scenarios. These scenarios differs in the reference input.

6.2.1 Evaluation with steering wheel

In the first scenario, the steering wheel unit mentioned in section 5.2.1 is employed to assess the performance and accuracy of the SBW system under realistic conditions.

During the measurement process, the steering wheel is initially rapidly rotated in both the right and left directions. Subsequently, the steering wheel is rotated slowly in both directions. The resulting measured values obtained from these actions are depicted in the figure presented below.
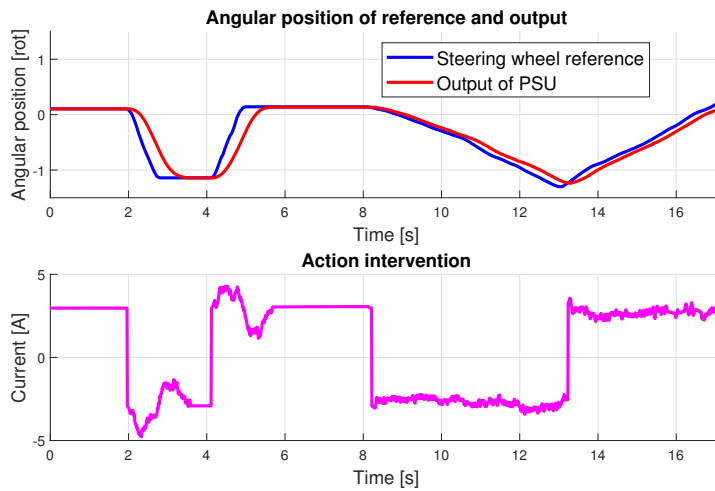
Figure 6.1: Evaluation of SBW unit using steering wheel reference
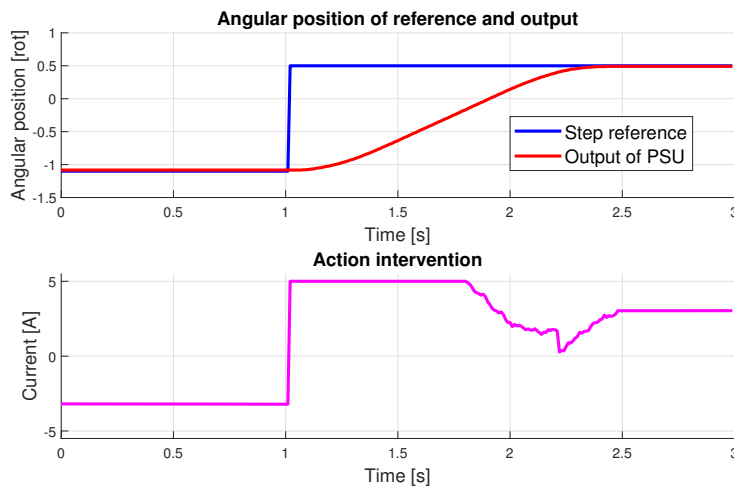
◼ 6.2.2 Step response evaluation

In the second scenario, a step of reference angle is applied to evaluate the response and behavior of the SBW unit in different driving scenarios. This allows for a comprehensive assessment of the SBW system's capabilities and performance in various operational conditions. The measured step response is depicted in figure below.

Figure 6.2: Evaluation of SBW unit using step reference

In contrast to the steering wheel scenario, the current output has been saturated, indicating the need to consider an increase in the maximum current output in future implementations.

6.3 Evaluation in simulation

In the single-track simulation, the thesis introduces three modes of rear axle control. The first mode involves conventional steering, where only the front axle is steered. The second mode is the antisymmetric steering, where the rear axle steering angle is the opposite of the front axle steering angle. The third mode is the symmetric mode, also known as the crab walk, where both the front and rear axles share the same steering angle.

Similar to the experimental evaluation, the simulation presents two scenarios. The first scenario involves a car making circles in a parking lot, while the second scenario simulates a vehicle transitioning from one traffic lane to another.

6.3.1 Parking lot scenario

In this scenario, the vehicle model undergoes circular motion with an approximate radius of 8 meters and a constant velocity of 1 meter per second. The figure presented below depicts a comparison between the conventional steering mode (Mode 1) and the antisymmetric steering mode (Mode 2).
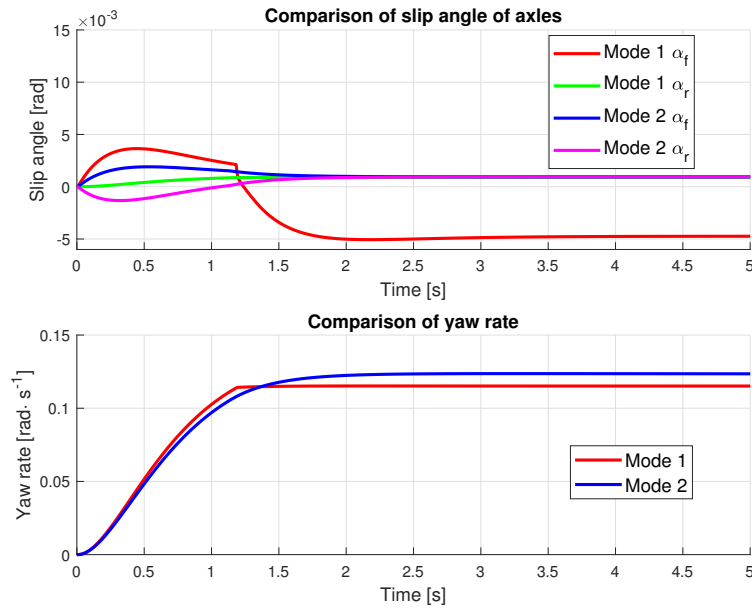

Figure 6.3: Parking lot circular motion scenario

The figure illustrates that employing an antisymmetric steering mode can generate an equivalent yaw rate while maintaining a considerably lower wheel slip angle. Consequently, this steering configuration has the potential to reduce tire wear substantially during parking and low-speed maneuvers.

33

An additional advantage of the antisymmetric mode is the increased yaw rate, which is particularly valuable during low-speed maneuvers or parking situations.

6.3.2 Highway scenario

In this simulation, the vehicle model travels at a speed of 30 meters per second and changes lanes by 3 meters within eight seconds. The comparison between the conventional steering mode (Mode 1) and the symmetric steering mode (Mode 3) in this scenario is illustrated below.
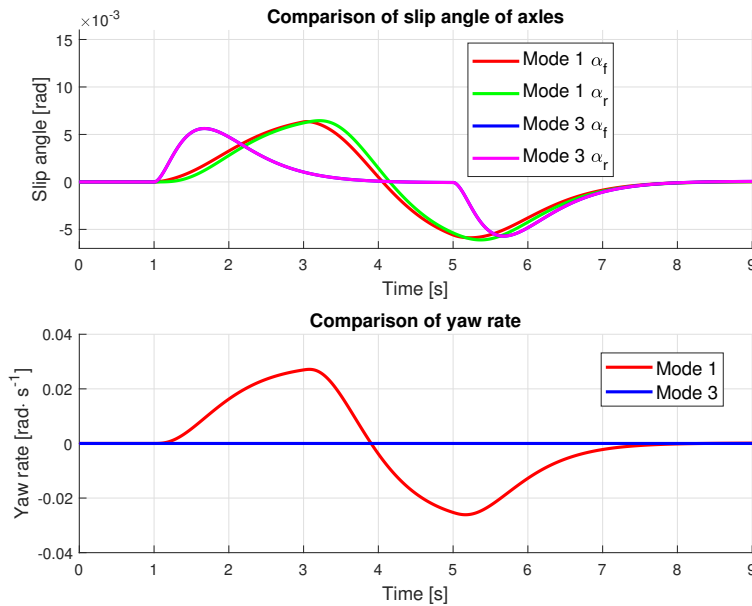
Figure 6.4: Highway traffic lane change scenario

This figure depicts an ideal situation where the yaw rate is maintained at zero throughout the maneuver, thanks to the use of symmetric steering. This can result in a significant increase in stability, particularly at higher speeds, such as on the highway. Additionally, the slip angle is maintained at lower values when employing symmetric steering. This can contribute to reduced tire wear, similar to what was observed in the first scenario.

34

Chapter 7

Conclusion

In conclusion, this bachelor's thesis has successfully achieved all of its stated goals, as outlined in the introduction.

Firstly, the objective to conduct a brief exploration of car dynamics was fulfilled by introducing the necessary physical quantities and principles alongside a single-track vehicle model.

Various mechanical steering systems were presented to provide a better understanding of vehicle steering. The introduction of the SBW concept, along with the latest approaches, revealed that SBW is an emerging technology that is increasingly being adopted in the mass-production of the automotive industry.

Furthermore, a SBW unit was implemented using an introduced hardware and successfully evaluated in two different scenarios.

Finally, simulations were conducted using the data obtained from the implemented SBW unit. These simulations effectively highlighted the advantages of the SBW concept and rear-axle steering.

This thesis has yielded promising results in terms of integrating SBW technology into the automotive industry.

7.1 Future work

Future work involves the potential integration of the implemented SBW unit into a demonstration vehicle for real-world testing. This would enable the collection and analysis of new and valuable data, thereby validating and promoting the adoption of the SBW technology.

Appendix A

Bibliography

[Bel20]   Jan Belák, *Advanced steering concept for overactuated vehicle*, Master's thesis, Czech technical university in Prague, 2020.

[Bha]   Utkarsh Bhardwaj, *The power steering and its different types explained*, The GoMechanic Blog.

[cita]   *Construction mechanic basic volume 02 - construction methods and practices*, Integrated publishing.

[citb]   *Electronic power steering*, Automotive electronics.

[citc]   *Getting to know rack and pinion steering*, The motor ombudsman.

[citd]   *Official lexus rz site.*

[Col21]   Danielle Collins, *What is friction compensation in servo control?*, Motion Control Tips (2021).

[Dav14]   Alex Davies, *Infiniti's new steering system is a big step forward—unless you love cars*, Wired (2014).

[Dru22]   Meghan Drummond, *Rack and pinion vs steering box systems*, Pony parts (2022).

[Efr20]   Denis Efremov, *Single-track model derivation*, Tech. report, Faculty of Electrical Engineering CTU, 2020.

[Fir22]   Firestone, *What's the difference between electric and hydraulic power steering?*, Firestone (2022).

[GFF06]   Abbas Emami-Naeini Gene F. Franklin, J. David Powell, *Feedback control of dynamic systems*, Pearson Education, 2006.

[Laz]   Orest Lazarowich, *Manual steering gear and linkage*, Lares Corporation.

[Pac02]   Hans B. Pacejka, *Tyre and vehicle dynamics*, Butterworth-Heinemann, 2002.

[Per23]   Chris Perkins, *How toyota is making the case for steer-by-wire*, Road and Track (2023).

[Pet20]   David Peterson, *Integral windup method in pid control*, Control Automation (2020).

[Reg21]   Suraj Regmi, *Gaussian smoothing in time series data*, Towards Data Science (2021).

BACHELOR'S THESIS ASSIGNMENT

I. Personal and study details

Student's name: **Dašek Filip**　　　　　　　　　Personal ID number: **499012**

Faculty / Institute: **Faculty of Electrical Engineering**

Department / Institute: **Department of Control Engineering**

Study program: **Cybernetics and Robotics**

II. Bachelor's thesis details

Bachelor's thesis title in English:

Vehicle steering systems development

Bachelor's thesis title in Czech:

Vývoj systému ízení vozu

Guidelines:

The primary goal of the thesis is to develop and implement vehicle steering system allowing for independent axles actuation.
The steering system will build on previously developed steer by wire concept.
1. Get familiar with vehicle dynamics and steering systems models and implement suitable model.
2. Get familiar with automotive electric power steering.
3. Develop and implement steer by wire system.
4. Evaluate developed steering system.

Bibliography / sources:

[1] Dieter Schramm, Manfred Hiller, Roberto Bardini – Vehicle Dynamics – Duisburg 2014
[2] Hans B. Pacejka - Tire and Vehicle Dynamics – The Netherlands 2012
[3] Robert Bosch GmbH - Bosch automotive handbook - Plochingen, Germany : Robet Bosch GmbH ; Cambridge, Mass.
: Bentley Publishers
[4] Rajamani R. (2012) Mean Value Modeling of SI and Diesel Engines. In: Vehicle Dynamics and Control. Mechanical
Engineering Series. Springer, Boston, MA. https://doi.org/10.1007/978-1-4614-1433-9_9

Name and workplace of bachelor's thesis supervisor:

doc. Ing. Tomáš Haniš, Ph.D.   Department of Control Engineering FEE

Name and workplace of second bachelor's thesis supervisor or consultant:

Date of bachelor's thesis assignment: **31.01.2023**　　　Deadline for bachelor thesis submission: **26.05.2023**

Assignment valid until:
by the end of summer semester 2023/2024

_____　　_____　　_____
doc. Ing. Tomáš Haniš, Ph.D.　　　　　　prof. Ing. Michael Šebek, DrSc.　　　　　prof. Mgr. Petr Páta, Ph.D.
Supervisor's signature　　　　　　　　　Head of department's signature　　　　　　　Dean's signature

III. Assignment receipt